Steady-State Recombining Plasma in a Radio-Frequency Plasma Device for Divertor-Detachment Study*)

Atsushi OKAMOTO, Hiroyuki TAKAHASHI, Yusuke KAWAMURA, Akira DAIBO, Takahiro KUMAGAI, Sumio KITAJIMA and Mamiko SASAO

Department of Quantum Science and Energy Engineering, Tohoku University, Sendai 980-8579, Japan

(Received 9 December 2011 / Accepted 12 February 2012)

Stable plasma production in a radio-frequency plasma source and steady-state high-neutral-pressure environment in a test region has been achieved simultaneously with backflow suppression components such as orifices and a differential pumping system. Neutral pressure in the test region is changed by two orders, resulting in changes in the electron temperature and density in the test region. Conversely, neutral pressure, electron temperature, and electron density near a plasma production region showed little change. The result indicates that the experimental device provides us independent control knobs of source plasma and neutral pressure in the test region.

Keywords: radio-frequency plasma production, divertor simulator, gas puffing, ion beam injection, backflow suppression

DOI: 10.1585/pfr.7.2401018

1. Introduction

Transient increase in high energy particle flux flowing into the divertor region, which is induced by the edge localized modes (ELMs), is a current topic in fusion reactor development. These high energy particles interact with ions and electrons in the divertor plasma. A concern is that the plasma density and temperature are then changed transiently [1], which reduces the recombination rate in the detached plasma [2–4]. To study the compatibility of the volumetric recombining processes with energetic ions caused by ELMs, a beam component injection that penetrates through a plasma source is a suitable method.

While a radio-frequency (RF) plasma source has the advantage of coexisting with energetic ion beams, sustaining suitable working pressure in a plasma production region is difficult over a wide range of neutral pressures in a recombining test region. In our previous experiments [5], a small amount of gas puffing was used to investigate an ion beam effect in ionizing plasma. Larger amounts of gas puffing changed the discharge mode, a result of backflow of the secondary gas to a plasma production region. To sustain a steady-state recombining plasma, larger amounts of the secondary gas will be required in the test region. Therefore, a stable plasma produced in the RF source should coexist with a steady-state high-neutral-pressure environment in the test region with the aid of suppressing the backflow of the secondary gas.

In this study, development of steady-state plasma production coexisting with a high-neutral-pressure region is presented. Orifices and a differential pumping system have been designed and installed as described in Sec. 2. Experimental results on the backflow suppression and characteristics of the plasma in the source and in the test region are shown in Sec. 3, followed by a summary in Sec. 4.

2. Experimental Setup

2.1 Plasma production and diagnostics

Experiments were performed in a linear plasma device, originally designed as a "Diagnostic Tool Assisted by Linear Plasma device for Helium Atom beam (DTALPHA)" [6]. A schematic of the experimental setup is shown in Fig. 1. The vacuum chamber consists of a quartz pipe (36 mm in diameter) coupling an antenna to a plasma at $z = 0.6$ m, and a main chamber (63 mm in diameter) made of stainless steel, where z is taken along the device axis and its origin is at the end of the chamber. To exclude complex molecular processes, helium was selected as the working gas for plasma production and secondary gas puffing. The working gas for plasma production is injected from a tube adjacent to the aperture, while the secondary gas for the recombining process study is injected from the downstream port ($z = 1.6$ m). A converging axial magnetic field up to 0.2 T is applied at the downstream port. An RF power supply of 13.56 MHz is used for the plasma production. The forward RF power is about 2 kW. Variable capacitors in a matching box are adjusted to minimize the RF power reflection in a specific gas puffing condition; the adjustment is fixed during pressure scanning experiments. Therefore the RF reflection power slightly changes with the neutral pressure but is still less than 0.3 kW.

author's e-mail: atsushi.okamoto@qse.tohoku.ac.jp

*) This article is based on the presentation at the 21st International Toki Conference (ITC21).

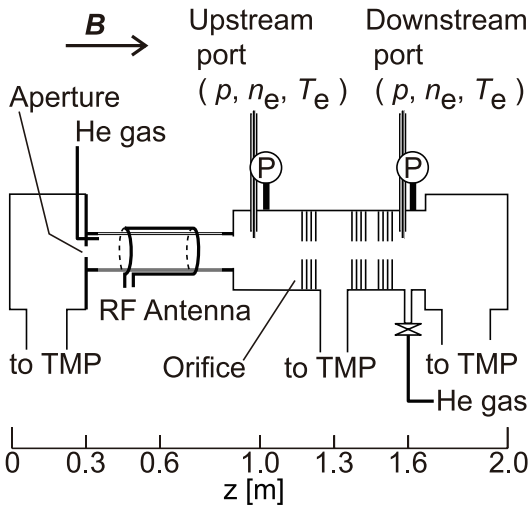

Fig. 1 Schematic of the experimental setup.

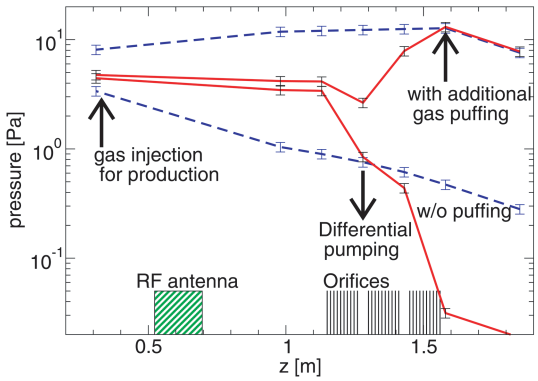

Fig. 2 Pressure profile along the device axis. Solid lines represent pressure profiles with orifices and a differential pumping system; dashed lines, without orifices and a differential pumping system. In each configuration, upper lines correspond to the case with additional gas puffing; lower lines, without it. Error bars resulting from dimensional accuracy for conductance calculations are shown.

Ionization gauges and single/double Langmuir probes are installed at the upstream port ($z = 1.0$ m) and downstream port to measure neutral pressure, electron density, and electron temperature. An emission collection optic is also installed at the upstream port. Atomic helium lines (He I), 667.8 nm ($2^1P - 3^1D$) and 726.1 nm ($2^1P - 3^1S$), are measured to obtain the electron density. The line intensity ratio measured by the experiment is compared with that obtained by a collisional radiative model [7, 8]. The line intensity ratio varies with electron density but is insensitive to the electron temperature [9].

2.2 Design of backflow suppression components

To suppress pressure variation in the plasma production region resulting from the secondary gas injection, three sets of 10 orifices ($z = 0.8 - 1.2$ m) and a differential pumping port ($z = 1.0$ m) were designed and installed in the DT-ALPHA device.

Neutral pressure profiles along the chamber axis have been calculated in the molecular flow condition, as shown in Fig. 2. In the calculation, a constant flow rate (0.17 Pa m^3/s) of helium, which corresponds to the experimental condition for plasma production, is supplied from the gas injection tube adjacent to the upstream aperture. When the pressure at the downstream port ($z = 1.6$ m) is about 0.1 Pa from the secondary gas puffing, pressure variation near the RF antenna is determined. While the pressure variation almost reaches one order for the case without the orifices and the differential pumping system, it is suppressed within 20% of the original pressure for the case with those components. In these calculations, the interval and the inner diameter of the orifices are 12 mm and 20 mm, respectively. The orifices reduce the conductance of a 0.15-m-long section of the chamber from 0.4 to 0.01 m^3/s. A turbo molecular pump with a pumping speed of 0.05 m^3/s is used in the differential pumping system.

On the basis of the calculation results, orifices with the same interval and inner diameter as assumed in the calculation have been installed. A turbo molecular pump has also been installed at the differential pumping port. Each set of orifices installed in the chamber consists of an inner ring made of stainless steel and a polytetrafluoroethylene outer support. The orifices are electrically isolated from the chamber potential and are kept in the floating potential.

3. Results and Discussion

For plasma production experiments, a pressure variation was determined. The working gas was injected at a constant flow rate (0.17 Pa m^3/s), while the secondary gas injection rate was varied. The relationship between the pressure measured at the upstream port and that at the downstream port is shown in Fig. 3. The upstream pressure, which is an index of the pressure in the plasma production region, increases slightly as the downstream pressure increases. The variation of the upstream pressure is larger in the experiment than in the calculation (Fig. 2). This is because the calculation is performed under the molecular flow condition, while our operation is in the transition regime rather than in the ideal molecular flow regime. However, the variation of the upstream pressure is successfully suppressed within one order, while the downstream pressure change is in the range of more than two orders.

Plasma parameters were measured for various flow rates of the secondary gas and for a constant flow rate of the working gas. The pressure dependence of the electron density measured at the upstream port is shown in Fig. 4. The electron density deduced from the ratio of He I line emission intensities agrees well with that obtained from the Langmuir probe characteristics. The electron density n_e at the upstream port is over 10^{18} m^{-3} in a wide range of down-

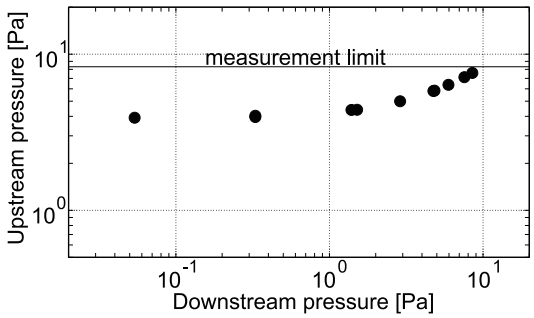

Fig. 3 Upstream pressure as a function of downstream pressure. Filled circle represents experimental results.

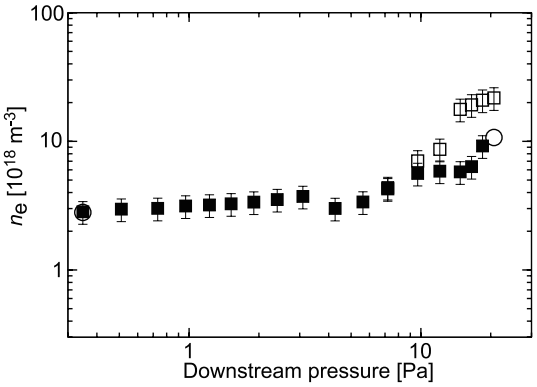

Fig. 4 Electron density measured at $r = 0$ at the upstream port as the function of neutral pressure p at the downstream port. Filled squares represent the electron density deduced from the ratio of He I line emission intensities for the matching condition optimized at $p = 0.3$ Pa; open squares, the same method but the matching condition optimized at $p = 21$ Pa; circles, from the Langmuir probe characteristics for reference.

stream pressures, 0.3–21 Pa. By optimizing the matching condition for the highest pressure case (open squares), we can achieve $n_e = 2 \times 10^{19}$ m^{-3}. For the matching condition optimized at $p = 0.3$ Pa (filled squares), the variation of n_e is suppressed within a factor of three over the wide range of downstream pressure. Comparison of Fig. 4 with Fig. 3 reveals that the variation in the electron density is consistent with that of the neutral pressure at the upstream port. Moreover, the plasma is stable during a discharge, suggesting that the backflow suppression components support steady-state plasmas in the RF plasma source in the secondary gas puffing experiment.

The pressure dependences of the electron temperature and density measured at the test region are shown in Fig. 5. The horizontal axis represents the neutral pressure measured at the test region. When the pressure increases from 0.3 to 18 Pa, the electron temperature monotonically decreases from 12 to 4 eV for the matching condition optimized at $p = 0.3$ Pa (filled circles). By optimizing the matching condition for the highest pressure case (open circles), $T_e = 2$ eV is achieved.

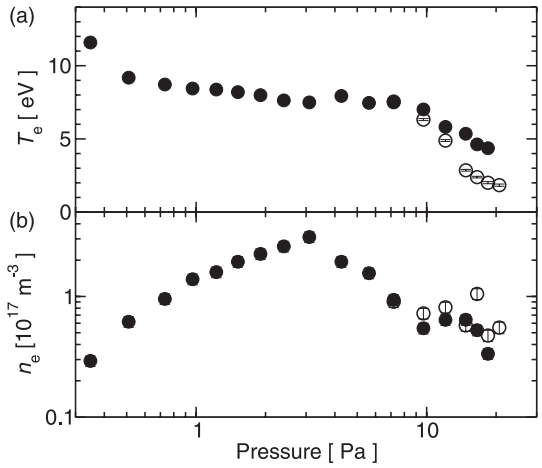

Fig. 5 (a) Electron temperature and (b) electron density measured at $r = 0$ at the downstream port as functions of the neutral pressure at the downstream port. Filled circles are obtained for the matching condition optimized at $p = 0.3$ Pa; open circles, for the matching condition optimized at $p = 21$ Pa.

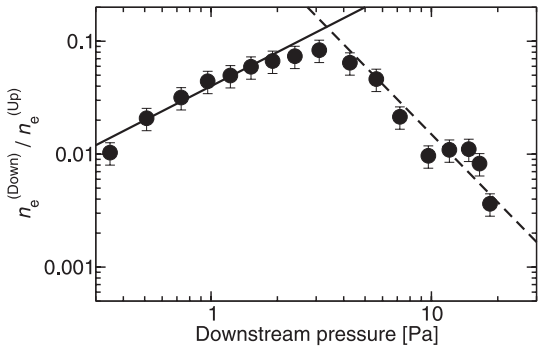

Fig. 6 Neutral pressure dependence of the ratio of electron density measured at the downstream port $n_e^{(Down)}$ to that at the upstream port $n_e^{(Up)}$. The matching condition is optimized at $p = 0.3$ Pa. Solid line represents a function that is proportional to p, while dashed line represents a function that is proportional to p^{-2}.

The electron density increases from 3×10^{16} m^{-3} to 3×10^{17} m^{-3} when the pressure increases from 0.3 to 3 Pa. Above $p \geq 3$ Pa, the electron density decreases to 3×10^{16} m^{-3} as the pressure increases. In the low pressure region (below $p \leq 3$ Pa), the increase in the electron density is considered to result from the electron collision ionization in the test region. Because the variation of the electron temperature is small, the ionization frequency is proportional to the neutral density. In the high pressure region (over $p \geq 3$ Pa), a possible process causing the decrease in the electron density is diffusion loss.

The ratio of the downstream density to the upstream density is shown in Fig. 6. A linear dependence of the density ratio on the downstream pressure is observed in the low pressure region, suggesting that ionization occurs in the test region as well as in the production region. In the

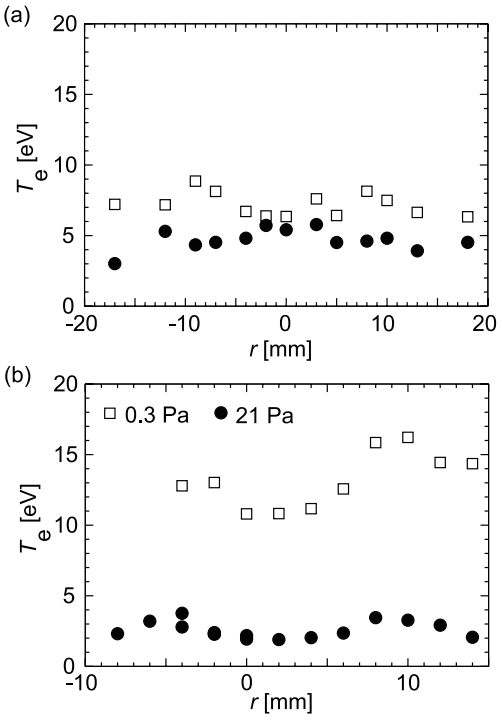

Fig. 7 Spatial distribution of electron temperature for different neutral pressures measured at (a) the upstream port and (b) the downstream port. Open squares represent p = 0.3 Pa at the downstream port; filled circles, 21 Pa.

high pressure region, the ratio decreases with p^{-2} slope. Understanding the p^{-2} dependence of the density ratio is our future work.

Radial profiles of the electron temperature at the upstream port and the downstream port are almost uniform as shown in Fig. 7. While the pressure at the downstream port changes from 0.3 to 21 Pa, the upstream pressure changes little as shown in Fig. 3. The electron temperature at the upstream port is about 5 eV and is almost unchanged against the downstream pressure as shown in Fig. 7 (a). Conversely, the electron temperature at the downstream port (Fig. 7 (b)) decreases to a few electron-volts as the pressure increases. The electron densities at the upstream port show similar profiles between the two pressures. An increase of approximately a factor of three is observed in the density profile, which is explained as an increase of a factor of three in the neutral density and the almost constant electron temperature.

4. Summary

Stable plasma production in an RF source and a steady-state high-neutral-pressure environment in a test region have been achieved simultaneously with backflow suppression components such as orifices and a differential pumping system. The neutral pressure in the test region is changed by two orders, resulting in changes in the electron temperature and density in the test region. Conversely, the neutral pressure, the electron temperature, and the electron density at the upstream port near the plasma production region changed little. The result indicates that the experimental device provides us the independent control knobs of upstream plasma and neutral pressure in the test region. This environment is promising for quantitative studies related to steady-state production of recombining plasmas and those interactions with transient ion beams.

Acknowledgements

This work was partly supported by the Ministry of Education, Culture, Sports, Science and Technology of Japan (MEXT) Grant-in-Aid for Young Scientists (B), 22740357.

[1] N. Ohno, D. Nishijima, S. Takamura, Y. Uesugi, M. Motoyama, N. Hattori, H. Arakawa, N. Ezumi, S. Krasheninnikov, A. Pigarov and U. Wenzel, Nucl. Fusion **41**, 1055 (2001).
[2] S.I. Krasheninnikov, A.Y. Pigarov, D.A. Knoll, B. LaBombard, B. Lipschults, D.J. Sigmar, T.K. Soboleva, J.L. Terry and F. Wising, Phys. Plasmas **4**, 1638 (1996).
[3] S. Kado, S. Kajita, Y. Iida, B. Xiao, T. Shikama, D. Yamasaki, T. Oishi and S. Tanaka, Plasma Sci. Technol. **6**, 2451 (2004).
[4] A. Okamoto, S. Kado, K. Sawada, Y. Kuwahara, Y. Iida and S. Tanaka, J. Nucl. Mater. **363-365**, 395 (2007).
[5] A. Okamoto, H. Takahashi, S. Kitajima and M. Sasao, Plasma Fusion Res. **6**, 1201153 (2011).
[6] A. Okamoto, T. Isono, T. Nishiuchi, H. Takahashi, S. Kitajima and M. Sasao, Plasma Fusion Res. SERIES **9**, 428 (2010).
[7] M. Goto, J. Quant. Spectrosc. Radiat. Transf. **76**, 331 (2003).
[8] T. Fujimoto, J. Quant. Spectrosc. Radiat. Transf. **21**, 439 (1979).
[9] B. Schweer, G. Mank, A. Pospieszczyk, B. Brosda and B. Pohlmeyer, J. Nucl. Mater. **196-198**, 174 (1992).